

<https://doi.org/10.1038/s41534-024-00862-5>

Contextual quantum metrology

Jeongwoo Jae^{1,2,5}, Jiwon Lee^{1,5}, M. S. Kim³, Kwang-Geol Lee¹✉ & Jinhyoung Lee^{1,4}✉

We demonstrate that the contextuality of measurement selection can enhance the precision of quantum metrology with a simple linear optical experiment. Contextuality is a nonclassical property known as a resource for various quantum information processing tasks. Recent studies show that contextuality by anomalous weak values can be utilized to enhance metrological precision, unraveling the role of contextuality in quantum metrology. Our contextual quantum metrology (coQM) scheme can elevate the precision of the optical polarimetry as much as 6 times the precision limit given by the Quantum Fisher Information. We achieve the contextuality-enabled enhancement with two mutually complementary measurements, whereas, in the conventional method, some optimal measurements to achieve the precision limit are either theoretically challenging to find or experimentally infeasible to realize. These results highlight that the contextuality of measurement selection is applicable in practice for quantum metrology.

Precision measurement has played a crucial role in the development of natural science and engineering since measurement is a means for observing nature. As a technology for precision measurement, quantum metrology has recently drawn attention with a wide range of applications such as microscopy¹, imaging^{2,3}, patterning^{4,5}, gravitational wave detection^{6–8}, and timekeeping^{9,10}. Quantum metrology enables measurements going beyond the precision of the standard quantum limit which can be obtained from the most-classical state in quantum physics. One of the resources for precision enhancement is entanglement, a nonclassical property of quantum states^{11–14}. However, an entangled state can easily lose its property through interaction with other objects, while the interaction is inevitable in metrology. This makes it challenging to generate and manipulate an entangled state. Due to the limitations, it is difficult in practice to attain the entanglement-enabled enhancement of precision. If easy-to-implement resources for metrology are found, the performance of quantum metrology can be greatly enhanced, as well as its practicality. In this work, we demonstrate that the contextuality of measurement selection¹⁵, another nonclassical property, is an easy-to-implement resource for quantum metrology.

Specifically, contextuality here refers to the dependency of quantum systems on measurement context¹⁶. Unlike classical predictions, quantum predictions for a given measurement can change depending on whether another measurement is performed simultaneously or not. Bell–Kochen–Specker theorem first showed that quantum physics is contextual^{17,18}, and this has been experimentally proved on various quantum systems^{19–22}. Also, it has been revealed that contextuality can be a resource for quantum information processing tasks such as quantum key distribution^{23,24}, universal quantum

computing²⁵, quantum state discrimination²⁶, and quantum machine learning^{27,28}. Recent studies show that contextuality caused by a post-selection and weak measurement can be utilized to enhance metrological precision^{29–31}. These works have fueled research directions to unravel the role of contextuality in quantum metrology.

To demonstrate the precision enhancement from the contextuality of measurement selection, we propose a method in quantum metrology which we call contextual quantum metrology (coQM). Unlike conventional quantum metrology, the coQM utilizes two measurement settings and their contextuality. In our experiment, we adopt an optical polarimetry devised to measure the concentration of sucrose solution³² and modify its scheme for the coQM. Our experiment employs two polarization measurements in mutually unbiased (or complementary) bases, and their selection context is implemented by toggling a polarizing beam splitter ‘in’ and ‘out’ from its optical path. Our setup is scalable in that the size of the experiment does not increase along with the increase of the number of probe photons. Also, the enhanced precision is attainable without error correction or mitigation which requires overhead^{33,34}. We finally show that the precision of coQM can go beyond the precision limit of conventional quantum metrology^{35–37} by a factor of 1.4–6.0.

Results

Contextual quantum metrology

Figure 1 shows an experimental schematic for the coQM. Here, the coQM estimates the concentration of sucrose solution by following four steps: preparing a polarized single photon as a probe light (see “Methods”), interacting the photon with the sucrose solution, measuring the polarization, and calculating an estimate via maximum likelihood estimator (MLE)

¹Department of Physics, Hanyang University, Seoul 04763, Republic of Korea. ²R&D center, Samsung SDS, Seoul 05510, Republic of Korea. ³Blackett Laboratory, Imperial College London, London SW7 2AZ, UK. ⁴Center for Quantum Simulation, Korea Institute of Science and Technology (KIST), Seoul 02792, Republic of Korea. ⁵These authors contributed equally: Jeongwoo Jae, Jiwon Lee. ✉ e-mail: kglee@hanyang.ac.kr; hyoung@hanyang.ac.kr

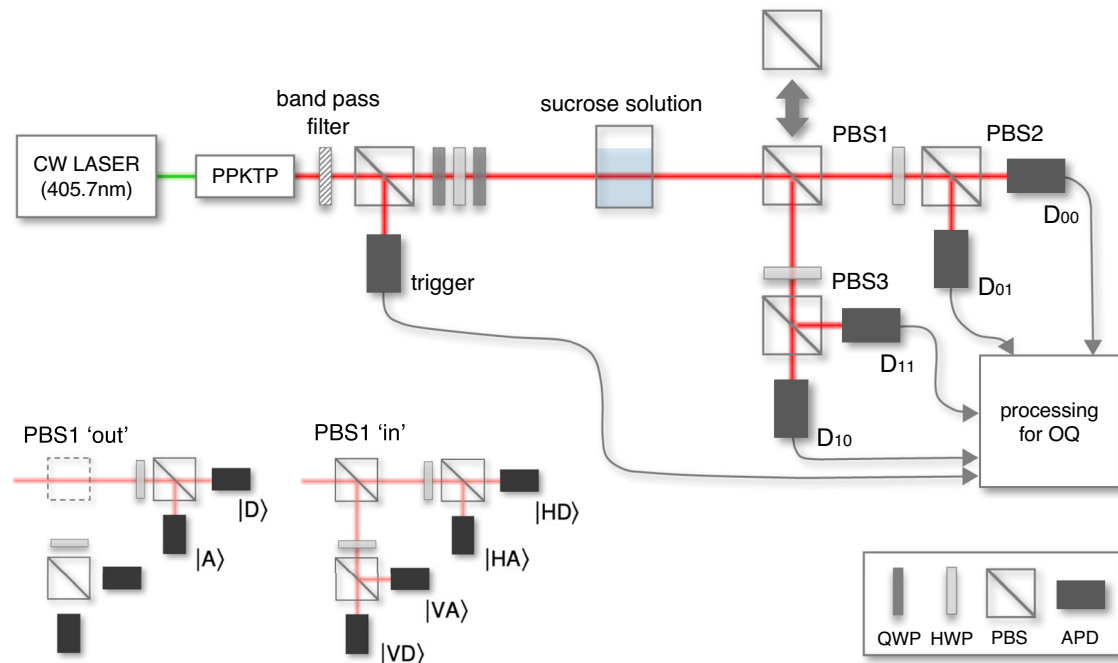


Fig. 1 | An experimental schematic for coQM. Our probe state is a polarization state of a heralded single-photon source (see “Methods”). The probe polarization rotates by angle $\alpha l c$ when it propagates through the sucrose solution, where $\alpha \approx 34.1$ deg ml dm⁻¹ g⁻¹ is the specific rotation of the sucrose solution, $l = 0.1$ dm is the traveling length of light in the solution, and c g ml⁻¹ is the concentration of the solution. We estimate the concentration c by measuring the polarization change. Here, we consider two measurement settings A and B , where A measures polarization in H/V basis and B does in a D/A basis tilted 45° from the basis of A by half-wave plate (HWP). For triggered events, the probabilities of the polarization bases are determined from relative counts of four avalanche photodiodes (APDs), D_{00} ,

D_{01} , D_{10} , and D_{11} . When polarizing beam splitter PBS1 is “out”, the measurement setup corresponds to the B measurement, and the counts on D_{00} and D_{01} determine probabilities of $|D\rangle$ and $|A\rangle$, respectively. When the PBS1 is “in”, the measurement setup corresponds to the consecutive measurement performing A first and B later, and the counts of D_{00} , D_{01} , D_{10} , and D_{11} represent joint probabilities of $|HD\rangle$, $|HA\rangle$, $|VD\rangle$, and $|VA\rangle$, respectively. We combine measuring data to construct operational quasiprobability (OQ) in Eq. (1), and an estimate is calculated with the maximum likelihood estimator of OQ in Eq. (2). The coQM utilizes the context of selecting the measurement A to enhance its precision. Experimental results in Fig. 2 demonstrate the enhancement.

using the operational quasiprobability which will be discussed later as in Eq. (1). The photon interacts with the sucrose solution as it propagates through the solution. Afterwards, the photon polarization rotates by angle $\alpha c l$, where α , c , and l are the specific rotation of the sucrose solution, the concentration of the solution, and the traveling length of light in the solution, respectively³². We can decide the concentration by measuring the polarization change for a given specific rotation and traveling length. All the procedures here look similar to those of the conventional quantum metrology³⁸, but the measurement and the estimation are steps that differentiate the coQM from the conventional approach.

In the measurement step, the coQM employs two different polarization measurement settings A and B to utilize the contextuality of measurement selection therefrom¹⁵. A measures the polarization in a specific basis $\{|H\rangle, |V\rangle\}$ and B does in a basis $\{|D\rangle, |A\rangle\}$ tilted 45° from the basis of A by half-wave plate. (Note that the measurements are incompatible as their observable operators σ_z and σ_x do not commute, $[\sigma_z, \sigma_x] \neq 0$.) Our basic setup is the measurement by B , and we consider a context of whether measurement A is selected to be performed or not, prior to performing B . If A is not selected, the measurement B only is performed, and probability is given by $p(b|B)$ for a binary value b . If A is selected, the experimental setup runs the consecutive measurement performing A first and B later. In this case, probability is given by $p(a, b|A, B)$ for an outcome pair (a, b) , where a is a binary outcome of A . Probabilities of B depend on whether an earlier A is performed for incompatible measurements A and B . The probabilities of B when A is performed are unequal to those of B when A is not performed, i.e., $p(b|A, B) \neq p(b|B)$, where the marginal $p(b|A, B) = \sum_a p(a, b|A, B)$. We say they are “contextual” in the context of measurement selection¹⁵. This is reflected in the operational quasiprobability $w(a, b)$ in (1). We note that the term “contextual” or “contextuality” here is not derived from Spekkens’ contextuality¹⁶ or quantum contextuality by the Kochen–Specker theorem¹⁸.

(We will discuss that the contextuality of measurement selection stems from the incompatibility of measurements^{39,40}.) Our metrology utilizes the contextuality to enhance the precision of the polarimetry.

In the experiment (Fig. 1), the context of selecting A is established by toggling “in” the state of the polarizing beam splitter PBS1. Setting PBS1 “in”, the photon is consecutively measured by two measurements A of H/V and B of D/A . Their outcome pairs (a, b) are identified by the clicks of the APDs D_{ab} . When D_{ab} clicks, the outcome of A is a , and the one of B is b . We note that, as shown in Fig. 1, outcome a is determined by PBS1, while outcome b is by the subsequent PBS2 or PBS3; specifically, PBS2 and PBS3 are located 170 mm away from PBS1, much farther than the coherence length of single-photon source $L_c \approx 0.052$ mm (see “Methods”). In this regard, measurement A precedes B in time.

In the estimation step, we employ a statistical model, so-called operational quasiprobability^{41,42}, which is given by

$$w(a, b) = p(a, b|A, B) + \frac{1}{2} (p(b|B) - p(b|A, B)). \quad (1)$$

The context-free condition in our measurement setup is to assume that the prediction of measurement B is invariant under the context of selecting measurement A . This is called the condition of no-signaling in time, represented by $p(b|B) = p(b|A, B), \forall a, b$ ⁴³. The crucial property of the operational quasiprobability is that, for the context-free condition, w is reduced to the probability by the consecutive measurement, $w(a, b) = p(a, b|A, B), \forall a, b$. To the contrary, the quantum predictions violate the condition in general, $w(a, b) \neq p(a, b|A, B)$, and $w(a, b)$ can even be negative-valued^{41,42}.

The conventional quantum metrology estimates a physical parameter θ with an estimator based on a conditional probability $p(x|\theta)$ for a

data set $\{x_i\}_{i=1}^{N_s}$ (see Supplementary Note 1). In the coQM, the operational quasiprobability plays a role in the conditional probability for the two data sets $\mathbf{x}_B = \{b_i\}_{i=1}^{N_s}$ and $\mathbf{x}_{AB} = \{(a_i, b_i)\}_{i=1}^{N_s}$. In other words, the coQM calculates an estimate of polarization θ with a maximum likelihood estimator given by

$$\tilde{\theta} \text{ s.t. } \partial_{\theta} l_w(\theta | \mathbf{x}_B, \mathbf{x}_{AB}) = 0, \quad (2)$$

where $l_w(\theta | \mathbf{x}_B, \mathbf{x}_{AB})$ is a log-likelihood function for w (see “Methods”). The possible problem caused by this replacement is that w can be negative unlike the conditional probability, so that the log-likelihood function diverges. However, we find that w remains positive for some range of parameters. We focus on the case for w to be applicable to the log-likelihood function without the divergence problem. Finally, for an initial polarization θ_0 , we derive the estimate of concentration \tilde{c} from the polarization change as $\tilde{c} = (\tilde{\theta} - \theta_0)/\alpha l$.

Contextuality-enabled enhancement of precision

Our goal is to demonstrate the outperformance of the coQM over conventional quantum metrology. We employ the error of estimate $\Delta\theta$, the standard deviation that the estimate differs from the actual value, to quantify the performance of estimation. The smaller the error is, the more precise the estimate is.

As a baseline of performance, we take the conventional quantum metrology and its error given by quantum Fisher information (QFI) F_q , $\Delta\theta_q = 1/\sqrt{N_s F_q}$, where N_s is the number of samples. This is known as the lower bound of error in the conventional method. In the coQM, we propose contextual Fisher information (coFI) to quantify the performance of the coQM,

$$F_{co} := \sum_{a,b} w(a, b|\theta) \left(\frac{\partial \log w(a, b|\theta)}{\partial \theta} \right)^2. \quad (3)$$

In the asymptotic limit of $N_s \rightarrow \infty$, the error of the coQM $\Delta\theta_{co}$ approaches to $1/\sqrt{N_s F_{co}}$ (see Supplementary Note 2 for the asymptotic property and estimator of coFI).

The coQM gains precision enhancement over the conventional quantum metrology if

$$\Delta\theta_{co} < \frac{\Delta\theta_q}{\sqrt{2}}. \quad (4)$$

Our method uses the two data sets \mathbf{x}_B and \mathbf{x}_{AB} . If each data set collects N_s samples, the total number of samples is $2N_s$ in our method. Reduction factor $\sqrt{2}$ in the error by the conventional is introduced, assuming the conventional take $2N_s$ samples (which is equivalent to comparing F_{co} to $2F_q$).

We here suggest specific cases satisfying the criterion (4). Instead of a theoretical proof, we briefly summarize the theory behind the enhancement of precision by following arguments: For the non-contextual model, the operational quasiprobability $w(a, b|\theta)$ becomes the joint probability of the consecutive measurement $p(a, b|A, B)$. In this case, the coQM is reduced and equivalent to the conventional quantum metrology using the consecutive measurement so that the $\Delta\theta_{co}$ equals or larger than $\Delta\theta_q$ (see Supplementary Note 1). For the contextual model, conversely, $\Delta\theta_{co}$ can be smaller than $\Delta\theta_q$ (see ref. 40 for rigorous discussions). Figure 2a shows simulation results of the contextuality-enabled enhancement on the Bloch sphere.

We perform polarization estimation of θ with probe states prepared in $|\psi\rangle = \cos(\theta/2)|H\rangle + e^{i\phi} \sin(\theta/2)|V\rangle$ for $0.46\pi \leq \theta \leq 0.55\pi$ and $\phi = 0.15\pi$. For the probe states, the operational quasiprobability is given by $w(a, b|\theta) = (1 + (-1)^a \cos \theta + (-1)^b \sin \theta \cos \phi)/4$. We draw $N_s = 10^5$ samples for each data set to construct the operational quasiprobability and calculate an estimate with the estimator (2). For polarization estimation of θ , QFI $F_q = 1$, so the coQM gains the contextuality-enabled enhancement if

$\Delta\theta_{co} < \Delta\theta_q/\sqrt{2} = 1/\sqrt{2N_s} \approx 2.24 \times 10^{-3}$. The errors of the coQM are smaller than the error limit of the conventional quantum metrology for the whole selected range of θ (Fig. 2b). The worst case in our results has $\Delta\theta_{co} \approx 1.53 \times 10^{-3}$ around $\theta = \pi/2$, and the best case has $\Delta\theta_{co} \approx 3.7 \times 10^{-4}$ around each end of the range of θ . This demonstrates that our method elevates the precision of polarimetry by a factor of 1.4–6.0 from the limit of conventional quantum metrology.

We estimate sucrose solutions of three different concentrations $c = 0.1, 0.3$, and 0.5 g ml^{-1} . We prepare the probe state with initial parameters $\theta_0 = 0.5\pi$ and $\phi = 0.15\pi$. For each concentration, we repeat the estimation 10 times. The results (Fig. 2d) show that the errors of estimates by the coQM, Δc_{co} , are smaller than the minimum error by the conventional quantum metrology ($\approx 5.9 \times 10^{-2}$); For $c = 0.1, 0.3$ and 0.5 g ml^{-1} , the mean errors are $\approx 3.7 \times 10^{-2}, \approx 3.3 \times 10^{-2}$, and $\approx 2.8 \times 10^{-2}$, respectively. This illustrates that the coQM exceeds the conventional quantum metrology by a wide margin.

These results illustrate the precision enhancement with the two incompatible measurements in the simple linear optical setup, whereas the conventional quantum estimation method requires identifying an optimal measurement, which may often be experimentally challenging to implement in practice. We remark that the contextuality of measurement selection is an easy-to-implement resource to enhance the precision of optical polarimetry.

Discussion

The contextuality of measurement selection stems from the incompatibility of quantum measurements³⁹. In the scenario of the consecutive measurement, if the two measurements A and B commute, the consecutive measurement is de facto a single measurement; the probabilities $p(b|B)$ and $p(b|A, B)$ are equal, and the prediction for B is noncontextual. Otherwise, the prediction for measurement B depends on whether performing the first measurement A is contextual except for a case when the initial state is prepared in an eigenstate of A . Thus, measurement incompatibility is necessary for the contextuality of measurement selection. We experimentally verify that the measurements A and B are incompatible by testing complementarity⁴⁴ (see “Methods”).

The noncommutation of observable operators defines the incompatibility among measurements, represented by projection-valued measures (PVM), which we assume in the present work. The notion of incompatibility needs to be generalized if the representation of measurement is generalized to positive operator-valued measure (POVM). This generalization is required, for example, if one considers an open quantum system in a noisy environment. Non-joint measurability (non-JM) is one of the generalizations³⁹. The non-JM plays an important role in a contextuality^{45,46}, as does the noncommutativity⁴⁷. In fact, non-JM and the contextuality of measurement selection are also closely related as the negativity of operational quasiprobability is the necessary and sufficient condition for non-JM^{40,48}.

Recently, there were studies in a similar vein to the present work^{49,50}, showing that noncommutativity can be a resource for quantum metrology. However, their schemes employ a post-selection to discard unwanted measurement outcomes, so there is a tradeoff between success probability and Fisher information; success probability becomes small if Fisher information is large⁵¹. Quantum post-selected metrology, such as weak value amplification methods, share this matter^{52,53}. On the contrary, our method utilizes all of the measurement outcomes for the estimation^{41,42}, implying that the coQM is free from such tradeoff.

This work demonstrates that utilizing the contextuality of measurement selection can enhance the precision of measurement. The experiment attains precision beyond the limit of conventional quantum metrology^{36,37}. The coQM has advantages over the conventional method (see Supplementary Note 1): it can enhance the precision without optimizing the measurements if they are incompatible, and it works even without any entangled state of a probe that has been regarded as difficult to generate and manipulate. We use the heralded single-photon source to clearly show the

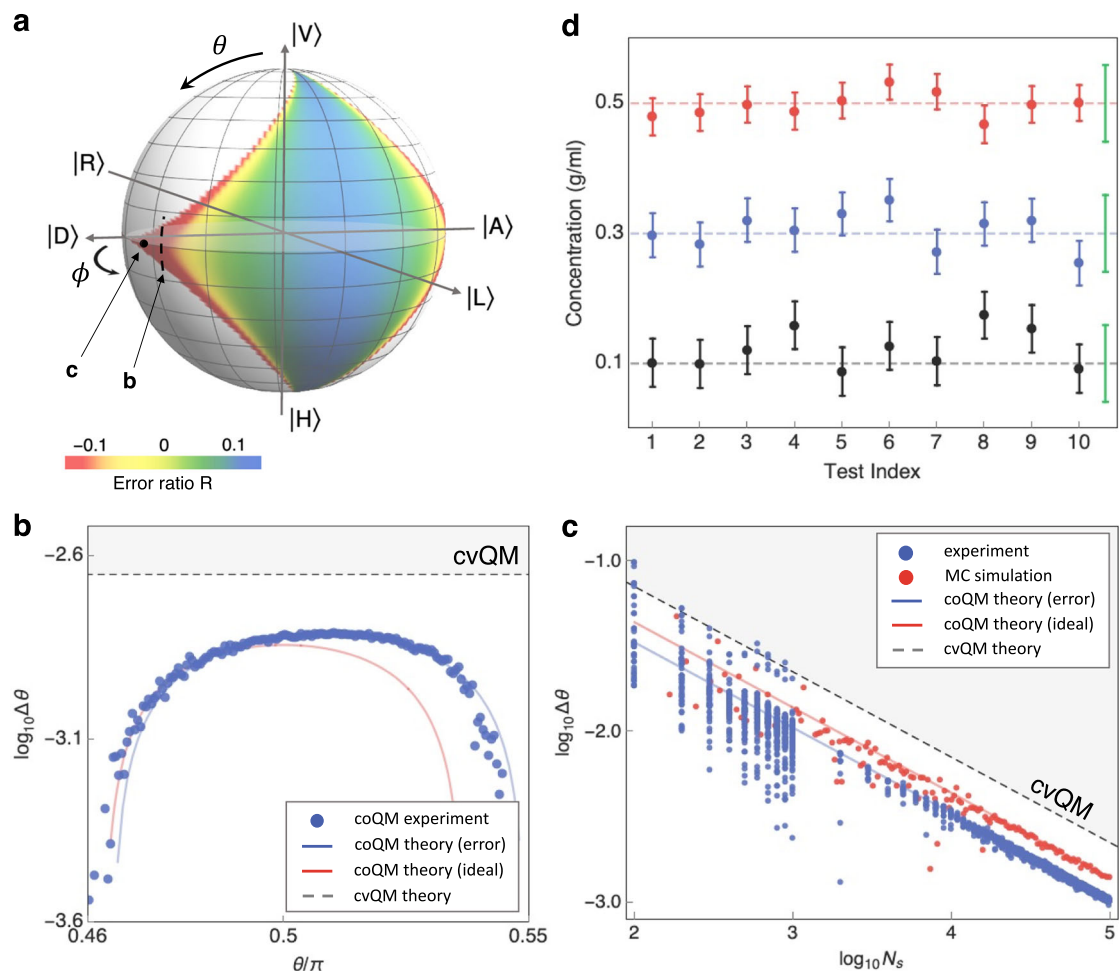


Fig. 2 | Simulation and experiment results of the coQM. **a** Landscape of error ratio of our $\Delta \theta_{co}$ to the conventional $\Delta \theta_q/\sqrt{2}$, $R := \log_{10}(\sqrt{2}\Delta \theta_{co}/\Delta \theta_q)$, on the Bloch sphere of a probe state $|\psi\rangle = \cos(\theta/2)|H\rangle + e^{i\phi}\sin(\theta/2)|V\rangle$, obtained by Monte-Carlo (MC) simulation. The coQM gains the contextuality-enabled enhancement if $R < 0$. The operational quasiprobability (OQ) is negative in the white regions. **b** Experiment results of θ estimation. We prepare the probe states, $|\psi\rangle$ s, by selecting 149 equiangular points from range $0.46\pi \leq \theta \leq 0.55\pi$ for a fixed $\phi = 0.15\pi$. For each probe state $|\psi\rangle$, we conduct θ estimation by drawing 10^5 samples ($N_s = 10^5$). Experiments (blue circles) assert that the coQM errors $\Delta \theta_{co}$ are smaller than the minimum error in the conventional quantum metrology (cvQM) $\Delta \theta_q/\sqrt{2} = 1/\sqrt{2N_s F_q}$ (dashed line), where quantum Fisher information $F_q = 1$. The red solid line is the theoretical prediction, assuming the ideal optical setup. We characterize the actual experimental setup by applying a systematic error model and use the

resultant model parameters to make the theoretical prediction (blue solid line) (see Supplementary Note 3). **c** Sample-size dependency of estimation error $\Delta \theta$. In the experiment, we prepare a probe state with $\theta = 0.5\pi$ and $\phi = 0.1\pi$. For small sample sizes, OQ can be negative by statistical fluctuation, which occasionally leads to estimation failures. For $N_s = 10^2$, the failure rate is 88%, whereas the failure rate becomes significantly low for larger sample sizes and it is negligible for $N_s \geq 7 \times 10^3$. **d** We estimate concentrations $c = 0.1, 0.3$, and 0.5 g ml^{-1} with a probe state $|\psi\rangle$ prepared with $\theta_0 = 0.5\pi$ and $\phi = 0.15\pi$. We draw $N_s = 10^5$ samples to estimate each concentration and repeat each estimation 10 times. The error of concentration Δc comes from that of polarization $\Delta \theta$ by $\Delta c = \Delta \theta/\alpha$. The error bar at each individual point represents Δc_{co} . The green error bar in each concentration represents the minimum error by the cvQM, $\Delta c_q/\sqrt{2}$.

performance of coQM per unit particle of probe. We expect that a multi-photon source can also be adopted for the coQM with similar settings of measurements¹⁵. Our method is expected to be applicable to a quantum sensor⁵⁴ if the context of measurement selection can be implemented within the sensor's system. In addition, the approaches employed to demonstrate the contextuality-enabled enhancements can be utilized to characterize quantum devices (see Supplementary Note 3), which is a fundamental task required to implement quantum technologies.

Methods

Heralded single photons

We generate the heralded single photon as follows. High energy pump photons ($p = 405.7 \text{ nm}$) from a continuous wave (CW) single mode laser (TOPMODE 405, TOPTICA) are sent to a periodically poled KTP (PPKTP) crystal. PPKTP splits the input photons into photon pairs (signal and idler photons) through the type-II spontaneous parametric down-conversion

(SPDC) process. The polarizations of signal and idler photons are orthogonal to each other so that a polarizing beam splitter (PBS) can separate them into two different optical paths. The idler photon is sent to an avalanche photodiode (APD) for triggering. The signal photon is sent to one of the four APDs (SPCM-QC4, Perkin Elmer). If the trigger APD is clicked, we count clicks on the four APDs. We control the count rate of the trigger APD to be $2 \times 10^5 \text{ cps}$ to sufficiently suppress multi-photon events, i.e., $|\text{SPDC}\rangle \approx |00\rangle + \epsilon|11\rangle$ for $\epsilon \ll 1$. The click signals are post-processed by a field programmable gate array (FPGA) with a time bin size of 25 ns. The wavelength λ and bandwidth $\Delta \lambda$ of the single-photon source are 810 nm and 2 nm, respectively. The coherence length is given by $L_c = \lambda^2/2\pi\Delta \lambda \approx 0.052 \text{ mm}$.

Input state preparation

We prepare an initial probe state by using a series of three wave plates (Fig. 1), one half-wave plate (HWP), and two quarter-wave plates (QWP).

After passing QWP₁, HWP, and QWP₂ sequentially, a horizontally polarized state $|H\rangle$ becomes an initial state

$$\begin{aligned} |\psi\rangle_{\text{in}} &= \text{QWP}_2\left(\frac{\pi}{4}\right)\text{HWP}(p)\text{QWP}_1(q)|H\rangle \\ &= e^{i(-2p+q+\pi/4)} \begin{pmatrix} \cos(\frac{\pi}{4}-q) \\ e^{i(4p-2q-\frac{\pi}{2})} \sin(\frac{\pi}{4}-q) \end{pmatrix}, \end{aligned} \quad (5)$$

where $p(q)$ is the angle of the fast axis of the half (quarter)-wave plate from the horizontal axis. The q value of QWP₂ is fixed at $\pi/4$. By adjusting the control parameters p and q to satisfy $\theta = \pi/2 - 2q$ and $\phi = 4p - 2q - \pi/2$, we finally obtain the parameterized state $|\psi\rangle_{\text{in}} = \cos(\theta/2)|H\rangle + e^{i\phi} \sin(\theta/2)|V\rangle$.

Test of complementarity

The measurements $A = \{\hat{A}_a\}$ and $B = \{\hat{B}_b\}$ are incompatible as their observable operators σ_x and σ_z do not commute, i.e., $[\sigma_x, \sigma_z] \neq 0$. These incompatible measurements are also said mutually complementary⁴⁴:

$$\text{Tr} \hat{A}_a \hat{B}_b = \frac{1}{2}, \forall a, b. \quad (6)$$

In our experiment, we test the complementarity through the probability of B after measuring A , $p(b|a) := p(a, b|A, B)/p(a|A, B)$. For the data used in Fig. 2b, the average of probability $p(b|a)$ is given by $p(0|0) = 0.4919$, $p(1|0) = 0.5081$, $p(0|1) = 0.4979$, and $p(1|1) = 0.5021$ with the error 2.4×10^{-3} .

Maximum likelihood estimator using operational quasiprobability

Maximum likelihood estimation is a method to find a parameter of a probability model which best describes observed data. This method assumes a likelihood function of the model, and maximizes the function to determine the most likely value in the parameter space as an estimate. In this work, we take the operational quasiprobability as the model depending on the phase θ .

For the two data sets \mathbf{x}_B and \mathbf{x}_{AB} , we define the log-likelihood function as

$$l_W(\theta|\mathbf{x}_B, \mathbf{x}_{AB}) := \frac{1}{N_s} \sum_{a,b=0}^1 N_W(a, b) \log w(a, b|\theta), \quad (7)$$

where $N_W(a, b) = N_{AB}(a, b) + (N_B(b) - N_{AB}(b))/2$. $N_B(b)$ is the number of counts for outcome b in the data set \mathbf{x}_B , and $N_{AB}(a, b)$ is the number of counts for outcome pair (a, b) in the data set \mathbf{x}_{AB} . $N_{AB}(b)$ is obtained by the marginal number of counts as $N_{AB}(b) = \sum_a N_{AB}(a, b)$. For a small number of samples, $N_W(a, b)$ can be negative by statistical fluctuations. We test whether the number count N_W is positive, and neglect cases where the count is negative. For small sample sizes, the OQ count $N_W(a, b)$ can be negative by statistical fluctuation, which occasionally leads to estimation failures. The experiment results in Fig. 2c show that the failure rate becomes significantly low for larger sample sizes, and it is negligible for $N_s \geq 7 \times 10^3$.

In a broader sense, the coQM proposes an approach of integrating the two different ensembles for single-parameter estimation. To show that our estimator $\hat{\theta}$ is unbiased and error of the estimate achieves Cramér–Rao bound^{55,56}, we propose a theory that describes the operational quasiprobability as an ensemble mixture model (see Supplementary Note 2).

Data availability

The data generated from the optical experiment are available from the authors upon reasonable request.

Code availability

The codes for the simulation of the optical experiment and the error analysis are available from the authors upon reasonable request.

Received: 18 December 2023; Accepted: 21 June 2024;

Published online: 04 July 2024

References

- Casacio, C. A. et al. Quantum-enhanced nonlinear microscopy. *Nature* **594**, 201–206 (2021).
- Treps, N. et al. Surpassing the standard quantum limit for optical imaging using nonclassical multimode light. *Phys. Rev. Lett.* **88**, 203601 (2002).
- Brida, G., Genovese, M. & Ruo Berchera, I. Experimental realization of sub-shot-noise quantum imaging. *Nat. Photonics* **4**, 227–230 (2010).
- Boto, A. N. et al. Quantum interferometric optical lithography: exploiting entanglement to beat the diffraction limit. *Phys. Rev. Lett.* **85**, 2733–2736 (2000).
- Parniak, M. et al. Beating the Rayleigh limit using two-photon interference. *Phys. Rev. Lett.* **121**, 250503 (2018).
- Abramovici, A. et al. Ligo: the laser interferometer gravitational-wave observatory. *Science* **256**, 325–333 (1992).
- Collaboration, T. L. S. A gravitational wave observatory operating beyond the quantum shot-noise limit. *Nat. Phys.* **7**, 962–965 (2011).
- Aasi, J. et al. Enhanced sensitivity of the ligo gravitational wave detector by using squeezed states of light. *Nat. Photonics* **7**, 613–619 (2013).
- Giovannetti, V., Lloyd, S. & Maccone, L. Quantum-enhanced positioning and clock synchronization. *Nature* **412**, 417–419 (2001).
- Pedrozo-Peñafiel, E. et al. Entanglement on an optical atomic-clock transition. *Nature* **588**, 414–418 (2020).
- Giovannetti, V., Lloyd, S. & Maccone, L. Quantum-enhanced measurements: beating the standard quantum limit. *Science* **306**, 1330–1336 (2004).
- Giovannetti, V., Lloyd, S. & Maccone, L. Quantum metrology. *Phys. Rev. Lett.* **96**, 010401 (2006).
- Giovannetti, V., Lloyd, S. & Maccone, L. Advances in quantum metrology. *Nat. Photonics* **5**, 222 (2011).
- Tan, K. C. & Jeong, H. Nonclassical light and metrological power: an introductory review. *AVS Quantum Sci.* **1**, 014701 (2019).
- Ryu, J. et al. Optical experiment to test negative probability in context of quantum-measurement selection. *Sci. Rep.* **9**, 19021 (2019).
- Spekkens, R. W. Contextuality for preparations, transformations, and unsharp measurements. *Phys. Rev. A* **71**, 052108 (2005).
- Bell, J. S. On the Einstein-Podolsky-Rosen paradox. *Physics* **1**, 195–200 (1964).
- Kochen, S. & Specker, E. P. The problem of hidden variables in quantum mechanics. *J. Math. Mech.* **17**, 59–87 (1967).
- Hasegawa, Y., Loidl, R., Badurek, G., Baron, M. & Rauch, H. Quantum contextuality in a single-neutron optical experiment. *Phys. Rev. Lett.* **97**, 230401 (2006).
- Kirchmair, G. et al. State-independent experimental test of quantum contextuality. *Nature* **460**, 494–497 (2009).
- Jerger, M. et al. Contextuality without nonlocality in a superconducting quantum system. *Nat. Commun.* **7**, 12930 (2016).
- Zhang, A. et al. Experimental test of contextuality in quantum and classical systems. *Phys. Rev. Lett.* **122**, 080401 (2019).
- Acín, A. et al. Device-independent security of quantum cryptography against collective attacks. *Phys. Rev. Lett.* **98**, 230501 (2007).
- Reichardt, B. W., Unger, F. & Vazirani, U. Classical command of quantum systems. *Nature* **496**, 456–460 (2013).
- Howard, M., Wallman, J., Veitch, V. & Emerson, J. Contextuality supplies the ‘magic’ for quantum computation. *Nature* **510**, 351–355 (2014).
- Schmid, D. & Spekkens, R. W. Contextual advantage for state discrimination. *Phys. Rev. X* **8**, 011015 (2018).
- Gao, X., Anschuetz, E. R., Wang, S.-T., Cirac, J. I. & Lukin, M. D. Enhancing generative models via quantum correlations. *Phys. Rev. X* **12**, 021037 (2022).

28. Anschuetz, E. R., Hu, H.-Y., Huang, J.-L. & Gao, X. Interpretable quantum advantage in neural sequence learning. *PRX Quantum* **4**, 020338 (2023).
29. Pusey, M. F. Anomalous weak values are proofs of contextuality. *Phys. Rev. Lett.* **113**, 200401 (2014).
30. Kunjwal, R., Lostaglio, M. & Pusey, M. F. Anomalous weak values and contextuality: robustness, tightness, and imaginary parts. *Phys. Rev. A* **100**, 042116 (2019).
31. Arvidsson-Shukur, D. R. M., McConnell, A. G. & Yunger Halpern, N. Nonclassical advantage in metrology established via quantum simulations of hypothetical closed timelike curves. *Phys. Rev. Lett.* **131**, 150202 (2023).
32. Yoon, S.-J., Lee, J.-S., Rockstuhl, C., Lee, C. & Lee, K.-G. Experimental quantum polarimetry using heralded single photons. *Metrologia* **57**, 045008 (2020).
33. Zhou, S., Zhang, M., Preskill, J. & Jiang, L. Achieving the Heisenberg limit in quantum metrology using quantum error correction. *Nat. Commun.* **9**, 78 (2018).
34. Maciejewski, F. B., Zimborás, Z. & Oszmaniec, M. Mitigation of readout noise in near-term quantum devices by classical post-processing based on detector tomography. *Quantum* **4**, 257 (2020).
35. Helstrom, C. W. Quantum detection and estimation theory. *J. Stat. Phys.* **1**, 231–252 (1969).
36. Holevo, A. S. *Probabilistic and Statistical Aspects of Quantum Theory* (North-Holland, Amsterdam, 1982).
37. Braunstein, S. L. & Caves, C. M. Statistical distance and the geometry of quantum states. *Phys. Rev. Lett.* **72**, 3439–3443 (1994).
38. Liu, J., Yuan, H., Lu, X.-M. & Wang, X. Quantum fisher information matrix and multiparameter estimation. *J. Phys. A* **53**, 023001 (2019).
39. Busch, P. Unsharp reality and joint measurements for spin observables. *Phys. Rev. D* **33**, 2253–2261 (1986).
40. Jae, J., Lee, J., Lee, K.-G., Kim, M. S. & Lee, J. Metrological power of incompatible measurements. Preprint at *arXiv* <https://doi.org/10.48550/arXiv.2311.11785> (2023).
41. Ryu, J., Lim, J., Hong, S. & Lee, J. Operational quasiprobabilities for qudits. *Phys. Rev. A* **88**, 052123 (2013).
42. Jae, J., Ryu, J. & Lee, J. Operational quasiprobabilities for continuous variables. *Phys. Rev. A* **96**, 042121 (2017).
43. Leggett, A. J. & Garg, A. Quantum mechanics versus macroscopic realism: is the flux there when nobody looks? *Phys. Rev. Lett.* **54**, 857–860 (1985).
44. Lee, J., Kim, M. S. & Brukner, C. Operationally invariant measure of the distance between quantum states by complementary measurements. *Phys. Rev. Lett.* **91**, 087902 (2003).
45. Tavakoli, A. & Uola, R. Measurement incompatibility and steering are necessary and sufficient for operational contextuality. *Phys. Rev. Res.* **2**, 013011 (2020).
46. Gühne, O., Haapasalo, E., Kraft, T., Pellonpää, J.-P. & Uola, R. Colloquium: incompatible measurements in quantum information science. *Rev. Mod. Phys.* **95**, 011003 (2023).
47. Budroni, C., Cabello, A., Gühne, O., Kleinmann, M. & Larsson, J.-A. Kochen-specker contextuality. *Rev. Mod. Phys.* **94**, 045007 (2022).
48. Jae, J., Baek, K., Ryu, J. & Lee, J. Necessary and sufficient condition for joint measurability. *Phys. Rev. A* **100**, 032113 (2019).
49. Arvidsson-Shukur, D. R. M. et al. Quantum advantage in postselected metrology. *Nat. Commun.* **11**, 3775 (2020).
50. Lupu-Gladstein, N. et al. Negative quasiprobabilities enhance phase estimation in quantum-optics experiment. *Phys. Rev. Lett.* **128**, 220504 (2022).
51. Combes, J., Ferrie, C., Jiang, Z. & Caves, C. M. Quantum limits on postselected, probabilistic quantum metrology. *Phys. Rev. A* **89**, 052117 (2014).
52. Ferrie, C. & Combes, J. Weak value amplification is suboptimal for estimation and detection. *Phys. Rev. Lett.* **112**, 040406 (2014).
53. Knee, G. C. & Gauger, E. M. When amplification with weak values fails to suppress technical noise. *Phys. Rev. X* **4**, 011032 (2014).
54. Degen, C. L., Reinhard, F. & Cappellaro, P. Quantum sensing. *Rev. Mod. Phys.* **89**, 035002 (2017).
55. Cramér, H. *Mathematical Methods Of Statistics* (Princeton University Press, 1946).
56. Rao, C. R. *Information and the Accuracy Attainable in the Estimation of Statistical Parameters. In Breakthroughs in Statistics.* (Springer Series in Statistics (Perspectives in Statistics). Springer, New York, NY, 1992).

Acknowledgements

MSK acknowledges the EPSRC grants (EP/T00097X/1 and EP/Y0047542/1), KIST Open Research Programme, and AppQInfo MSCA ITN from the European Union Horizon 2020. KGL was supported by the National Research Foundation of Korea (NRF) grant funded by the Korean government (MSIT) (No. 2023M3K5A109481312) and the Institute of Information and Communications Technology Planning & Evaluation (IITP) grant funded by the Korean government (MSIT) (No. 2022-0-01026). J.L. was supported by the National Research Foundation of Korea (NRF) grant funded by the Korea government (MSIT) (No. 2022M3E4A1077369), and Quantum Simulator Development Project for Materials Innovation(NRF-2023M3K5A1092818) through the National Research Foundation of Korea(NRF) funded by the Korean government (Ministry of Science and ICT(MSIT)).

Author contributions

Jeongwoo Jae, M. S. Kim, and Jinhyoung Lee contributed to the theoretical formulation of contextual quantum metrology. Jiwon Lee and Kwang-Geol Lee conducted the optical experiments and the data analysis. All authors contributed to discussions in this work. Jeongwoo Jae wrote the paper with the assistance of other authors. Jeongwoo Jae and Jiwon Lee contributed equally to this work.

Competing interests

The authors declare no competing interests.

Additional information

Supplementary information The online version contains supplementary material available at <https://doi.org/10.1038/s41534-024-00862-5>.

Correspondence and requests for materials should be addressed to Kwang-Geol Lee or Jinhyoung Lee.

Reprints and permissions information is available at <http://www.nature.com/reprints>

Publisher's note Springer Nature remains neutral with regard to jurisdictional claims in published maps and institutional affiliations.

Open Access This article is licensed under a Creative Commons Attribution 4.0 International License, which permits use, sharing, adaptation, distribution and reproduction in any medium or format, as long as you give appropriate credit to the original author(s) and the source, provide a link to the Creative Commons licence, and indicate if changes were made. The images or other third party material in this article are included in the article's Creative Commons licence, unless indicated otherwise in a credit line to the material. If material is not included in the article's Creative Commons licence and your intended use is not permitted by statutory regulation or exceeds the permitted use, you will need to obtain permission directly from the copyright holder. To view a copy of this licence, visit <http://creativecommons.org/licenses/by/4.0/>.

© The Author(s) 2024